Theory of the First-Order Raman Effect in Solid-State Plasmas in a Magnetic Field

E-Ni Foo* and N. Tzoar†
Department of Physics, The City College of the City University of New York, New York, New York 10031
(Received 25 July 1969)

The Raman scattering cross section in the forward direction has been calculated for narrow-gap semiconductors such as GaAs, GaP, etc. The main mechanism considered for the scattering is the "phonon fluctuations," while the negligible contribution to the scattering from electron-charge fluctuations has been omitted. Our result shows the possibility of observing ionic as well as electronic excitation modes resulting from the self-consistent field of the electron-phonon system.

I. INTRODUCTION

In recent years, Raman scattering from narrow-gap semiconductors has been studied extensively both theoretically and experimentally. It provides us with a fundamental method to study the elementary excitations and their interactions in solids. The measurements of the scattering cross section from weakly doped semiconductors such as GaAs,[1,2] InSb,[3,4] etc., allows us, by comparing the theoretical results with the experiments, to determine the deformation potential and the electro-optic coefficient—the coupling parameters of radiation with the systems. Many theoretical treatments considered either the photon-system coupling with a single-component one-band electron gas, omitting all phonon effects,[5–8] or else considered undoped semiconductors in which no conduction electron is present.[9–11] Raman scattering from plasmons and phonons in GaAs was recently reported and demonstrated the coupling between the longitudinal optic-phonon modes and the longitudinal plasma modes.[1,2] The results are in good agreement with theoretical predictions.[12,13] The scattering cross section was calculated phenomenologically for a real solid considering excitations of longitudinal optic phonons and plasmons. The scattering cross section from transverse phonons was estimated using the value of the integrated scattering cross section from undoped semiconductors. A microscopic calculation for an electron-phonon system has been reported.[14] However, it is also limited to longitudinal excitations. In this paper, we will present a macroscopic calculation of the Raman scattering cross section, in almost transparent semiconductors, which takes into account both longitudinal and transverse phonons, plasmons, or magnetoplasmons and their coupling to the radiation field.

In the scattering process, a well-collimated beam of monochromatic radiation is incident on an almost transparent solid. Subsequently, a small amount of the radiation is scattered into 4π sr. The light which comes off in some fixed direction is then analyzed in a spectrometer. The spectral distribution of the scattered radiation, along with an associated angular distribution, provides the basic information which is contained in this type of experiment. The scattering is completely characterized by the wave-vector transfer $\mathbf{k}=\mathbf{k}_1-\mathbf{k}_2$ and frequency transfer $\omega=\omega_1-\omega_2$ from the radiation field to the solid. Here, $\mathbf{k}_1(\mathbf{k}_2)$ and $\omega_1(\omega_2)$ are, respectively, the incident (scattered) wave vector and frequency. It is convenient to measure the scattering cross section at fixed k (or fixed scattering angle) and then to analyze the spectrum. The frequencies and intensities at resonances appearing in the spectrum give us the frequencies of elementary excitations and the coupling constants of the solid, respectively.

The calculations in this paper are restricted to the so-called first-order Raman effect[9] where a single elementary excitation, i.e., phonon, plasmon, or linear combination, thereof, is excited in the scattering process. The first-order Raman scattering can be produced by two processes. The first one is the "direct" coupling of the radiation field to the electron-density fluctuations, illustrated diagrammatically in Fig. 1. It has been considered by many authors,[5–8] and we can draw the following conclusion: In order to observe plasma collective modes, the wave-number transfer to the system, k, must be small relatively to the screening wave number k_D or k_{FT}. Also, the scattering cross section from electron-density fluctuations is proportional to $(k/k_{FT})^2$, which is negligible in the forward scattering.[8,15]

---

* Present address: Department of Physics, Temple University, Philadelphia, Pa. 19122.

† Research sponsored by the Air Force Office of Scientific Research Office of Aerospace Research, U. S. Air Force, under AFOSR Grant No. 69-1676.

[1] A. Mooradian and G. B. Wright, Phys. Rev. Letters **16**, 999 (1966).

[2] A. Mooradian and A. L. McWharter, Phys. Rev. Letters **19**, 849 (1967).

[3] R. E. Slusher, C. K. N. Patel, and P. A. Fleury, Phys. Rev. Letters **18**, 530 (1967).

[4] C. K. N. Patel and R. E. Slusher, Phys. Rev. Letters **22**, 282 (1969).

[5] P. M. Platzman, Phys. Rev. **139**, A379 (1965).

[6] P. M. Platzman, P. A. Wolff, and N. Tzoar, Phys. Rev. **174**, 489 (1968).

[7] P. A. Wolff, Phys. Rev. **171**, 436 (1968).

[8] P. A. Wolff, Phys. Rev. B **1**, 950 (1970).

[9] R. Loudon, Proc. Roy. Soc. (London) **275**, 218 (1963).

[10] R. Loudon, Advan. Phys. **13**, 423 (1964).

[11] O. Fano, Phys. Rev. **103**, 1202 (1956); J. J. Hopfield, *ibid.* **112**, 1555 (1958); C. H. Henry and J. J. Hopfield, Phys. Rev. Letters **15**, 964 (1965).

[12] A. L. McWhorter and P. N. Argyres, Bull. Am. Phys. Soc. **12**, 102 (1967).

[13] A. L. McWhorter, in *Physics of Quantum Electronics*, edited by P. L. Kelley, B. Lax, and P. E. Tannenwald (McGraw-Hill Book Co., New York, 1966), p. 111.

[14] P. M. Platzman and N. Tzoar, Phys. Rev. **182**, 510 (1969); Y. C. Lee and N. Tzoar, *ibid.* **140**, A396 (1965).

[15] E-Ni Foo and N. Tzoar, Phys. Rev. **185**, 644 (1969).

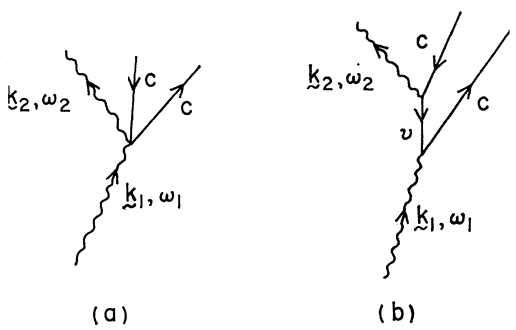

FIG. 1. Schematic description of the matrix element for Raman scattering produced by direct coupling of the radiation field to the electron-density fluctuations. Here, c and v indicate, respectively, the conduction band and valence bands.

The second process is the coupling of the radiation field to the so-called "phonon fluctuations," which was considered by Loudon for undoped semiconductors[9,10] and is shown pictorially in Fig. 2(a). The result was then generalized for doped semiconductors, including longitudinal optic phonons and plasmons.[12,13] For III-V compound semiconductors, the radiation field couples also to electron-density fluctuations indirectly via the electrooptic coefficient, the process shown by Fig. 2(b). Its scattering cross section is not proportional to k; therefore, it is the dominant term in the forward scattering, which is our main concern. In this paper, we calculate the first-order Raman scattering cross section induced by phonon fluctuations and the indirect electron-density fluctuations from doped semiconductors, applicable to the small-k case, in which coupling between phonons (both longitudinal and transverse), plasmons (or magnetoplasmons), and radiation fields is possible. Our result is, therefore, correct for forward scattering. For large-angle scattering, the contribution from direct electron-density fluctuations has also to be considered.

The semiconductors which have been investigated experimentally all have two atoms per unit cell and, therefore, possess three acoustic and three optic phonon-mode branches in the undoped system. We consider only the optic branches which have higher frequencies and are easier to resolve.

In Sec. II, the general expression for cross section is calculated macroscopically including both longitudinal and transverse excitations. In Sec. III, the general expression for cross section derived in Sec. II is applied to several cases of phonon-plasmon or magnetoplasmon interactions. The cross section from magnetoplasmon-polariton modes which has been reported experimentally will be discussed in detail. The scattering cross section from an anisotropic electron gas including phonon fluctuation will be treated in Sec. IV.

II. GENERAL FORMALISM OF THEORY

Raman scattering of light from a doped semiconductor involves the interaction between photons and both conduction and valence electrons. In undoped semiconductors, the photon can excite a phonon via electrons while leaving the electronic state unchanged if the phonon energy is smaller than the gap energy E_G. In a doped semiconductor, there is a continuum above the ground state; therefore, the photon can either excite a phonon, or else alter the conduction electron states, while leaving the valence electron states still unchanged in the final state. The single Raman scattering event via phonon fluctuations involves the destruction of an incident photon of frequency ω_1, the creation of a scattered photon of frequency ω_2, and the creation (Stokes) or destruction (anti-Stokes) of a phonon of frequency ω. This kind of scattering process is displayed pictorially in Fig. 2(a). It is expressed in terms of H_{ER} and H_{EL} which represent the electron-photon and electron-lattice interactions. The Hamiltonian of the electron-photon interaction H_{ER} is given by

$$H_{ER}=\frac{e}{m}\sum_j\sum_{\mathbf{k}}\left(\frac{2\pi\hbar}{\epsilon_\infty V\omega_{\mathbf{k}}}\right)^{1/2}\times(a_{\mathbf{k}}^{-}e^{i\mathbf{k}\cdot\mathbf{r}_j}+a_{\mathbf{k}}^{+}e^{-i\mathbf{k}\cdot\mathbf{r}_j})\hat{\epsilon}_{\mathbf{k}}\cdot\mathbf{p}_j, \quad (1)$$

where $a_{\mathbf{k}}^{+}$ and $a_{\mathbf{k}}^{-}$ are the photon creation and destruction operators, $\mathbf{p}_j$ and $\mathbf{r}_j$ are the momentum and position of the jth electron, ϵ_∞ is the optical dielectric constant, V is the crystal volume, and $\hat{\epsilon}_{\mathbf{k}}$ is the unit polarization vector of the photon having momentum $\mathbf{k}$.

Here we are interested in semiconductors with two atoms per unit cell. The relative displacement of the two sublattices produced by a long-wavelength optic phonon having polarization s and wave vector $\mathbf{k}$ is given by

$$\mathbf{U}(\mathbf{R})=(\hbar/2MN\omega_{s\mathbf{k}})^{1/2}\hat{\xi}_{s\mathbf{k}}e^{i\mathbf{k}\cdot\mathbf{R}}(b_{s-\mathbf{k}}^{+}+b_{s\mathbf{k}}^{-}), \quad (2)$$

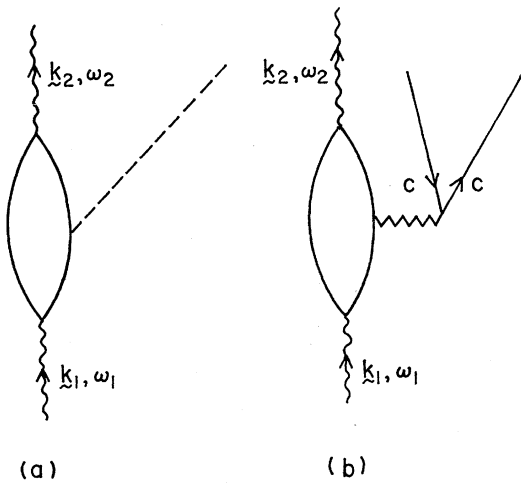

FIG. 2. Schematic description of the matrix element for Raman scattering due to phonon fluctuation. Here, (a) represents the process induced by electron-lattice interaction H_{EL} or H_{EL}'. The dash line represents the phonon final state. (b) represents the process induced by electron Coulomb interaction H_{EE}. Here, the zig-zag line is the Coulomb line and the final state is an electron-hole pair.

where $b_{s-\mathbf{k}}^{+}$ and $b_{s\mathbf{k}}^{-}$ are the phonon creation and destruction operators, M is the reduced mass of the two atoms, and N is the number of atoms in the crystal. The electron-lattice interaction H_{EL} is linear in the components U_i of the relative displacement, and its matrix element is written as[16]

$$(\alpha|H_{EL}|\beta)=\Xi_{\alpha\beta}{}^{i}\bar{U}_i/a, \tag{3}$$

where a is the lattice constant. The deformation potential $\Xi_{\alpha\beta}{}^{i}$ is the matrix element of the derivative of the perturbed periodic potential with respect to $\mathbf{U}_i$. Here, $\bar{U}_i$ is defined by $\mathbf{U}_i=\mathbf{U}_i e^{i\mathbf{k}\cdot\mathbf{R}}$ [see Eq. (2)].

In the III-V semiconductors, there exists also the so-called Fröhlich coupling which represents the interaction of the electrons with the charge of the optic vibration modes of a polar lattice. It can be expressed as[17]

$$H_{EL}{}'=\frac{ie}{k}\left(\frac{1}{\epsilon_\infty}-\frac{1}{\epsilon_0}\right)^{1/2}\left(\frac{2\pi\hbar\omega_l}{V}\right)^{1/2}e^{i\mathbf{k}\cdot\mathbf{R}}(b_{l-\mathbf{k}}{}^{+}+b_{l\mathbf{k}}{}^{-}), \tag{4}$$

where the subscript l in $b_{l\mathbf{k}}$ signifies the longitudinal optic phonon and ϵ_0 is the static dielectric constant. If we use ordinary perturbation theory and retain only the contributing terms of lowest order in k, the scattering matrix elements become

$$(\alpha|H_{EL}{}'|\beta)=ie\left(\frac{1}{\epsilon_\infty}-\frac{1}{\epsilon_0}\right)^{1/2}\left(\frac{2\pi\hbar\omega_i}{V}\right)^{1/2}\times N_{\alpha\beta}{}^{\mathbf{k}}(b_{l-\mathbf{k}}{}^{+}+b_{l\mathbf{k}}{}^{-}), \tag{5}$$

with

$$N_{\alpha\beta}{}^{\mathbf{k}}=\frac{\mathbf{p}_{\alpha\beta}{}^{\mathbf{k}}}{m(\omega_\alpha-\omega_\beta)}\quad\text{for }\alpha\neq\beta$$

$$=1\quad\text{for }\alpha=\beta,$$

where $\mathbf{p}_{\alpha\beta}{}^{\mathbf{k}}$ is the component of $\mathbf{p}_{\alpha\beta}$ in the direction of $\mathbf{k}$. The interband matrix element $\alpha\neq\beta$ of the Fröhlich coupling is much smaller than the intraband matrix element, their ratio being $r=k_1a$ for a two-band model.[14] For a number of important intraband processes, the matrix elements almost cancel and we must include the contribution from the interband terms as well.

Similar to the Fröhlich coupling, the Coulomb interaction between electrons, H_{EE}, can also cause scattering by exciting electron-hole pairs or plasmons. Its Hamiltonian is

$$H_{EE}=\sum_{\mathbf{k}}\frac{4\pi e^2}{k^2}(\rho_{\mathbf{k}}\rho_{-\mathbf{k}}-n). \tag{6}$$

Here $\rho_{\mathbf{k}}$ is the electron-density fluctuation operator $\rho_{\mathbf{k}}=\sum_j e^{i\mathbf{k}\cdot r_j}$ and n is the average electron density. Its

[16] G. L. Bir and G. E. Pikus, Fiz. Tverd. Tela **2**, 2287 (1960) [English transl.: Soviet Phys.—Solid State **2**, 2039 (1961)].
[17] H. Elrenreich, J. Phys. Chem. Solids **2**, 131 (1957).

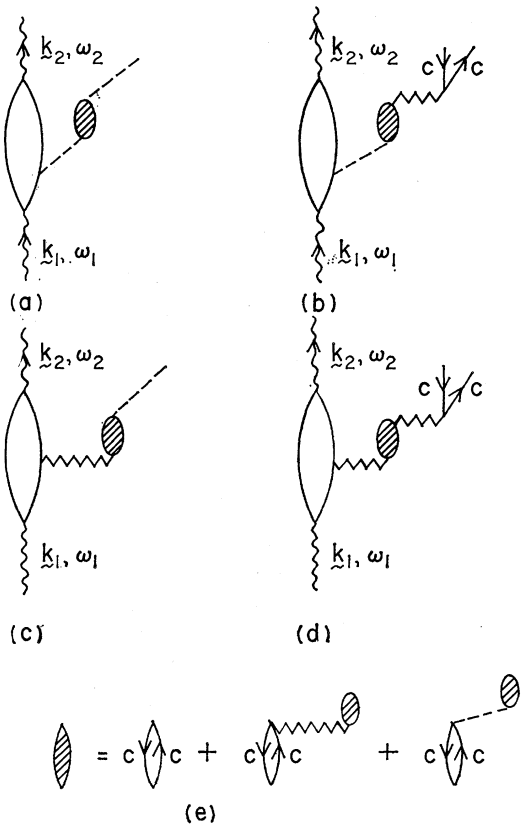

FIG. 3. Schematic description of the matrix element for Raman scattering due to phonon fluctuation including self-consistent field. Here, (a) and (b) represent the processes induced by H_{EL} or $H_{EL}{}'$, with a phonon and an electron-hole pair in the final states, respectively, and (c) and (d) are the processes induced by H_{EE} with a phonon and an electron-hole pair in the final states, respectively. (e) is the diagramatic representation of the self-consistent dielectric constant.

scattering matrix elements are similar to that of $H_{EL}{}'$:

$$(\alpha|H_{EE}|\beta)=\sum_{\mathbf{k}}\frac{4\pi e^2}{k}N_{\alpha\beta}{}^{\mathbf{k}}\rho_{\mathbf{k}}. \tag{7}$$

Here $N_{\alpha\beta}{}^{\mathbf{k}}$ is defined by Eq. (5). The difference between H_{EL} (or $H_{EL}{}'$) and H_{EE} is that H_{EL} (or $H_{EL}{}'$) either excites directly a phonon or else indirectly excites electron-hole pairs via the excited phonon, whereas H_{EE} excites only indirectly electron-hole pairs via Coulomb interaction. These two processes are illustrated pictorially in Fig. 2. For H_{EL} and $H_{EL}{}'$ [see Fig. 2(a)], the first interaction line attached to the main matrix element is a pure phonon line. For H_{EE} [see Fig. 2(b)], it is a Coulomb line. Subsequently, the phonon or the Coulomb couplings can excite electron-hole pairs and the excited electron-hole pairs can recombine to emit a phonon or to excite another electron-hole pair via Coulomb coupling, and so on to excite a plasmon. These "bubble chain" processes are illustrated pictorially in Fig. 3. This is the so-called "random-phase approximation."

In the initial and final states, the valence electronic states are fully occupied, while the conduction electrons may be in excited states. The virtual intermediate states involve the excitation of electron-hole pairs from the valence band. As illustrated in Fig. 2, the three interactions H_{ER}, H_{ER}, and H_{EL}' can occur in any time order, leading to six different processes. Loudon first obtained the Raman scattering tensor for undoped semiconductors by treating the three-step scattering process using third-order time-dependent perturbation theory. If only the deformation-potential coupling is considered, the scattering cross section is

$$\frac{d\sigma}{d\omega d\Omega}=\frac{r_0^2}{2\pi}\frac{(n_0+1)V}{a^2m^2MN\omega_0}|R_{12}{}^i|^2\delta(\omega-\omega_0), \tag{8}$$

where $r_0=e^2/mc^2$, ω_0 is the phonon frequency, and[9]

$$R_{12}{}^i=\frac{1}{V}\sum_{\alpha,\beta}\left(\frac{p_{0\beta}{}^2p_{\beta\alpha}{}^1\Xi_{\alpha 0}{}^i}{(\omega_\beta+\omega_0-\omega_1)(\omega_\alpha+\omega_0)}+\text{five terms}\right), \tag{9}$$

which is the Raman scattering tensor. For doped semiconductors, the cross section given by Eq. (8) has to be modified to include the effect of conduction electrons.[14] The quantities $R_{12}{}^i$ are only weakly dependent on the presence of conduction electrons. The conduction electrons exclude a small set of states around the band minimum from the scattering process. The occupation of these states must be taken into account in the intermediate-state sums. When ω_1 is not close to E_G (gap energy), then it is clear that the correction is of order E_F/E_G. However, the phonon occupation number n_0+1 is severely modified in the presence of conduction electrons. For convenience, one can rewrite Eq. (8) in the following form:

$$\frac{d\sigma}{d\omega d\Omega}=\frac{r_0^2}{2\pi}\frac{V|R_{12}{}^i|^2}{a^2m^2MN\omega_0}\times|(n_0+1|b_{-\mathbf{k}}{}^+{+}b_{\mathbf{k}}{}^-|n_0)|^2\delta(\omega-\omega_0). \tag{10}$$

To obtain Eq. (10), we have used the relation (for undoped semiconductors)

$$(n_0+1|b_{-\mathbf{k}}{}^+{+}b_{\mathbf{k}}{}^-|n_0)=(n_0+1)^{1/2}. \tag{11}$$

In doped semiconductors, Eq. (11) is no longer valid and we have to calculate the matrix element $\langle b_{-\mathbf{k}}{}^+{+}b_{\mathbf{k}}{}^-\rangle$ including the motion of conduction electrons and the coupling with photons self-consistently. It is convenient to write Eq. (10) as

$$\frac{d\sigma}{d\omega d\Omega}=\frac{r_0^2}{2\pi}\frac{V|R_{12}{}^i|^2}{a^2m^2MN\omega_{s\mathbf{k}}}\times\int_{-\infty}^{\infty}\langle[b_{s-\mathbf{k}}{}^+(t)+b_{s\mathbf{k}}{}^-(t)][b_{s-\mathbf{k}}{}^+(0)+b_{s\mathbf{k}}{}^-(0)]\rangle e^{i\omega t}dt. \tag{12}$$

Since the phonon operators are related to the lattice polarization operator $\mathbf{P}$ by

$$\mathbf{P}=\left(\frac{Ne^2h}{2M\omega_{s\mathbf{k}}}\right)^{1/2}\hat{\xi}_{s\mathbf{k}}e^{i\mathbf{k}\cdot\mathbf{R}}(b_{s-\mathbf{k}}{}^+{+}b_{s\mathbf{k}}{}^-), \tag{13}$$

the scattering cross section can be expressed in terms of the polarization-polarization correlation function as

$$\frac{d\boldsymbol{\sigma}}{d\omega d\Omega}=\frac{r_0^2}{2\pi}\frac{V^2|R_{12}{}^i|^2}{a^2m^2M^2e^2}\int_{-\infty}^{\infty}\langle\mathbf{P}(t)\mathbf{P}(0)\rangle e^{i\omega t}dt. \tag{14}$$

Here $d\boldsymbol{\sigma}/d\omega d\Omega$ is a tensor which depends on the polarization vectors of the incident and the scattered light. The polarization-polarization correlation function is analogous to the electron-density correlation function for an electron gas. We shall follow a similar procedure as that used in calculating the electron-density correlation function to calculate the polarization correlation function. It is usually most convenient to determine the closely-related response function (the lattice polarizability) χ_p. In thermal equilibrium, χ_p is related to the correlation function through the dissipation fluctuation theorem[18]:

$$\begin{aligned}\int_{-\infty}^{\infty}&\langle\mathbf{P}(t)\mathbf{P}(0)\rangle e^{i\omega t}\\&=\frac{1}{e^{\beta\omega}-1}\mathrm{Im}\left(\int_0^{\infty}\langle[\mathbf{P}(t),\mathbf{P}(0)]\rangle e^{i\omega t}dt\right)\\&\equiv\frac{1}{e^{\beta\omega}-1}\mathrm{Im}\chi_p.\end{aligned} \tag{15}$$

Substituting Eq. (15) into Eq. (14), the scattering cross section can be written as

$$\frac{d\boldsymbol{\sigma}}{d\omega d\Omega}=\frac{r_0^2}{2\pi}\frac{1}{e^{\beta\omega}-1}\frac{V^2|R_{12}{}^i|^2}{a^2m^2M^2e^2}\mathrm{Im}\chi_p. \tag{14'}$$

The polarizability χ_p can be calculated macroscopically and has a well-known simple physical interpretation. It determines the lattice polarization induced in the solid by an external polarizing field of wave vector $\mathbf{k}$ and frequency ω:

$$\mathbf{P}=\chi_p\cdot\mathbf{E}_{\text{ext}}. \tag{16}$$

The polarizability χ_p must then be calculated self-consistently, including conduction electrons and photons. Therefore, the full Maxwell equations, the equation of motion of the lattice, and the electrons have to be considered simultaneously.

The lattice polarizability χ_p can be evaluated using the macroscopic theory of the optic mode of diatomic

[18] D. N. Zubarev, Usp. Fiz. Nauk **71**, 71 (1960) [English transl.: Soviet Phys.—Usp. **3**, 320 (1960)].

crystals developed by Born and Huang.[19] The equation of motion of the lattice is

$$\mathbf{u}+\omega_t^2\mathbf{u}-[(\epsilon_0-\epsilon_\infty)/4\pi]^{1/2}\omega_t\mathbf{E}_{\text{total}}=0, \quad (17)$$

where $\mathbf{u}=\mathbf{U}/(MN)^{1/2}$. Here $\mathbf{E}_{\text{total}}$ is the total electronic field which is the sum of the external electric field $\mathbf{E}_{\text{ext}}$ and the induced electric field $\mathbf{E}_{\text{ind}}$, and ω_t is the transverse phonon frequency. The polarization $\mathbf{P}$ is related to $\mathbf{u}$ and $\mathbf{E}_{\text{total}}$ by

$$\mathbf{P}=[(\epsilon_0-\epsilon_\infty)/4\pi]^{1/2}\omega_t\mathbf{u}+[(\epsilon_\infty-1)/4\pi]\mathbf{E}_{\text{total}}. \quad (18)$$

The induced electric and magnetic field components $\mathbf{E}_{\text{ind}}$ and $\mathbf{H}_{\text{ind}}$ of the radiation field, the lattice polarization $\mathbf{P}$, and the electronic current $\mathbf{J}$ are related by Maxwell's equations:

$$\nabla\times\mathbf{H}_{\text{ind}}=\frac{1}{c}\left(\frac{\partial\mathbf{E}_{\text{ind}}}{\partial t}+4\pi\frac{\partial\mathbf{P}}{\partial t}+4\pi\mathbf{J}\right),$$
$$\nabla\times\mathbf{E}_{\text{ind}}=-\frac{1}{c}\frac{\partial\mathbf{H}_{\text{ind}}}{\partial t}. \quad (19)$$

The electron current and the lattice polarization are additionally related to the electric field by means of Ohm's law. The relations are

$$\mathbf{J}=\boldsymbol{\sigma}\cdot\mathbf{E},$$
and
$$\mathbf{P}=(1/4\pi)\boldsymbol{\alpha}\cdot\mathbf{E}. \quad (20)$$

Here $\boldsymbol{\sigma}$ is the electronic conductivity, which is related to the electronic dielectric tensor $\boldsymbol{\epsilon}$ via the relation

$$\boldsymbol{\epsilon}=\mathbf{I}+(4\pi/i\omega)\boldsymbol{\sigma}, \quad (21)$$

and $\boldsymbol{\alpha}$ is the lattice polarizability for an empty lattice, given by

$$\boldsymbol{\alpha}=-\frac{\omega_l^2-\omega_t^2}{\omega(\omega-i\eta)-\omega_t^2}\mathbf{I}, \quad (22)$$

where $\omega_l^2=\omega_t^2\epsilon_0/\epsilon_\infty$ is the frequency of the longitudinal phonon and η is the phenomenological phonon collision frequency. In doped semiconductors, the polarization will be affected by the presence of conduction electrons. We shall treat the conduction electrons in the random-phase approximation, i.e., the electrons are considered to be noninterating particles but the response is calculated using the induced fields self-consistently. In using Eqs. (20) one must choose the "correct" electric field which corresponds to the proper response function. Thus, when considering the electron-lattice coupling, i.e., H_{EL} or H_{EL}' [see Eqs. (3) and (4)], the $\mathbf{E}_{\text{ext}}$ is polarizationlike, which induces directly only a polarization field (not an electron current). This, in turn, via Maxwell's equations, will produce an induced electric field $\mathbf{E}_{\text{ind}}$. The induced electric field then drives both polarization fluctuations and an electron current. Therefore, the polarization field is the response to the total electric current, but the electronic current responds only to the induced electric field. The relations of Eqs. (20) become

$$\mathbf{J}=\boldsymbol{\sigma}\cdot\mathbf{E}_{\text{ind}}$$
and
$$\mathbf{P}=(1/4\pi)\boldsymbol{\alpha}\cdot(\mathbf{E}_{\text{ind}}+\mathbf{E}_{\text{ext}}). \quad (20')$$

From Eqs. (19) and (20), we can obtain the relation between $\mathbf{E}_{\text{ind}}$ and $\mathbf{E}_{\text{ext}}$ as

$$\mathbf{E}_{\text{ind}}=(\omega^2/c^2)\mathbf{D}\cdot\boldsymbol{\alpha}\cdot\mathbf{E}_{\text{ext}}, \quad (23)$$

where

$$\mathbf{D}^{-1}=k^2\mathbf{I}-\mathbf{kk}-(\omega^2/c^2)(\boldsymbol{\epsilon}+\boldsymbol{\alpha}). \quad (24)$$

Equations (20') and (23) yield

$$\mathbf{P}=(1/4\pi)\boldsymbol{\alpha}\cdot[(\omega^2/c^2)\mathbf{D}\cdot\boldsymbol{\alpha}+\mathbf{I}]\cdot\mathbf{E}_{\text{ext}}, \quad (25)$$

and the polarizability χ_p now becomes

$$\chi_p{}^i=(1/4\pi)\hat{\xi}_i\cdot\boldsymbol{\alpha}\cdot[(\omega^2/c^2)\mathbf{D}\cdot\boldsymbol{\alpha}+\mathbf{I}]\cdot\hat{\xi}_i. \quad (26)$$

Substituting χ_p from Eq. (26) into Eq. (15), the scattering cross section becomes

$$\left(\frac{d\sigma}{d\omega d\Omega}\right)_i=\frac{r_0^2}{2\pi}\frac{|V_D|^2}{e^{\beta\omega}-1}\frac{1}{4\pi}\operatorname{Im}\left[\hat{\xi}_i\cdot\boldsymbol{\alpha}\cdot\left(\frac{\omega^2}{c^2}\mathbf{D}\cdot\boldsymbol{\alpha}+\mathbf{I}\right)\cdot\hat{\xi}_i\right], \quad (27)$$

where

$$V_D=VR_{12}{}^i/amNe.$$

The cross section given by Eq. (27) is the correct expression for scattering from transverse mode. When the longitudinal modes in III-V semiconductors are considered, an additional contribution due to the Frölich coupling has to be taken into account. The Fröhlich coupling includes both electron-lattice coupling H_{EL}' and electron-electron Coulomb coupling H_{EE}. For undoped semiconductors, one needs only consider the contribution from H_{EL}' and the scattering cross section from longitudinal mode [Eq. (27)] should be modified as

$$\left(\frac{d\sigma}{d\omega d\Omega}\right)_l=\frac{r_0^2}{2\pi}\frac{|V_D+V_F|^2}{e^{\beta\omega}-1}\frac{1}{4\pi}$$
$$\times\operatorname{Im}\left[\hat{\xi}_l\cdot\boldsymbol{\alpha}\cdot\left(\frac{\omega^2}{c^2}\mathbf{D}\cdot\boldsymbol{\alpha}+\mathbf{I}\right)\cdot\hat{\xi}_l\right], \quad (28)$$

where

$$V_F=iep_{12}{}^{\mathbf{k}}/m^2$$

and

$$p_{12}{}^{\mathbf{k}}=\frac{1}{V}\sum_{\alpha\neq\beta}\left(\frac{p_{0\beta}{}^2p_{\beta\alpha}{}^1p_{\alpha0}{}^{\mathbf{k}}}{(\omega_\beta+\omega_l-1)(\omega_\alpha+\omega_l)\omega_\alpha}+\text{five terms}\right). \quad (29)$$

For doped semiconductors, one has to consider also the contribution from Coulomb coupling H_{EE}. To treat the scattering due to Coulomb coupling, one calculates

[19] M. Born and K. Huang, *Dynamical Theory of Crystal Lattices* (Clarendon Press, Oxford, 1954).

the electron-density–density correlation function instead of the polarization-polarization function. The scattering cross section is given by

$$\left(\frac{d\sigma}{d\omega d\Omega}\right)_{\text{Coulomb}} = \frac{r_0^2}{2\pi}\frac{|V_F|^2}{e^{\beta\omega}-1}\left(\frac{4\pi e^2}{k}\right)^2 \times\int_0^\infty \langle[\rho_{\mathbf{k}}(t),\rho_{\mathbf{k}}(0)]\rangle e^{i\omega t}dt = \frac{r_0^2}{2\pi}\frac{|V_F|^2}{e^{\beta\omega}-1}\int_0^\infty \langle[J_l(t),J_l(0)]\rangle e^{i\omega t}dt, \tag{30}$$

where

$$J_l(t)=(4\pi e/ik)\rho_{\mathbf{k}}(t).$$

Here, the subscript l represents the longitudinal component. To calculate the electronic-current response, we follow a similar procedure as that used in calculating the lattice-polarization response. The electronic-current response function χ_J is defined as

$$J_l=\chi_J E_l \tag{31}$$

and the corresponding cross section is

$$\left(\frac{d\sigma}{d\omega d\Omega}\right)_{\text{Coulomb}} = \frac{r_0^2}{2\pi}\frac{|V_F|^2}{e^{\beta\omega}-1}\,\text{Im}\chi_J. \tag{32}$$

Now the external electric field is chosen to be "electronic-current-like," which can produce directly the electronic longitudinal current (not the lattice-polarization field). The electronic current, in turn, generates an induced electric field which will produce both electronic current and lattice-polarization fluctuations. Thus, the electronic current $\mathbf{J}$ is the response to the total electric field, but the lattice polarization $\mathbf{P}$ is one response only to the induced electric field. The relations become

$$\mathbf{J}=\boldsymbol{\sigma}\cdot(\mathbf{E}_{\text{ind}}+\mathbf{E}_{\text{ext}})$$

and

$$\mathbf{P}=(1/4\pi)\boldsymbol{\alpha}\cdot\mathbf{E}_{\text{ind}}. \tag{20''}$$

From Eqs. (19) and (20''), one can obtain the relation between $\mathbf{E}_{\text{ind}}$ and $\mathbf{E}_{\text{ext}}$, which is

$$\mathbf{E}_{\text{ind}}=(\omega^2/c^2)\mathbf{D}(4\pi/i\omega)\cdot\boldsymbol{\sigma}\cdot\mathbf{E}_{\text{ext}}. \tag{33}$$

Substituting Eq. (33) into Eq. (20''), one obtains

$$\mathbf{J}=\boldsymbol{\sigma}\cdot[(\omega^2/c^2)\mathbf{D}\cdot(4\pi/i\omega)\boldsymbol{\sigma}+\mathbf{I}]\cdot\mathbf{E}_{\text{ext}}, \tag{34}$$

and the response function χ_J becomes

$$\chi_J=\hat{\xi}_l\cdot\boldsymbol{\sigma}\cdot[(\omega^2/c^2)\mathbf{D}\cdot(4\pi/i\omega)\boldsymbol{\sigma}+\mathbf{I}]\cdot\hat{\xi}_l. \tag{35}$$

Substituting χ_J of Eq. (35) into the cross-section expression Eq. (32) yields

$$\left(\frac{d\sigma}{d\omega d\Omega}\right)_{\text{Coulomb}} = \frac{r_0^2}{2\pi}\frac{|V_F|^2}{e^{\beta\omega}-1} \times\text{Im}\left[\hat{\xi}_l\cdot\left(\frac{4\pi}{i\omega}\right)\boldsymbol{\sigma}\cdot\left(\frac{\omega^2}{c^2}\mathbf{D}\cdot\left(\frac{4\pi}{i\omega}\boldsymbol{\sigma}\right)+\mathbf{I}\right)\cdot\hat{\xi}_l\right]. \tag{36}$$

To calculate the total scattering cross section from longitudinal modes, one has to consider the contributions from both the deformation potential H_{EL}, which induces phonon fluctuations, and the electrooptic coefficient $H_{EL}'+H_{EE}$, which induces both phonon and electron-density fluctuations, as well as their cross terms. The total response function can be derived by following a similar procedure to that used in calculating χ_p and χ_J. The only modification is to replace Eqs. (20) by

$$\mathbf{J}=\boldsymbol{\sigma}\cdot(\mathbf{E}_{\text{ind}}+\mathbf{E}_{\text{ext}}),$$
$$\mathbf{P}=(1/4\pi)\boldsymbol{\alpha}\cdot(\mathbf{E}_{\text{ind}}+\mathbf{E}_{\text{ext}}), \tag{20'''}$$

for the electrooptic coefficient part. The total cross section is now obtained in the form

$$\left(\frac{d\sigma}{d\omega d\Omega}\right)_l = \frac{r_0^2}{2\pi}\frac{1}{e^{\beta\omega}-1}\frac{1}{4\pi}\,\text{Im}\left\{\hat{\xi}_l\cdot\left[(V_D+V_F)^2\boldsymbol{\alpha} +V_F^2(\boldsymbol{\varepsilon}-\mathbf{I})+\frac{\omega^2}{c^2}((V_D+V_F)\boldsymbol{\alpha}+V_F(\boldsymbol{\varepsilon}-\mathbf{I}))\cdot\mathbf{D} \cdot((V_D+V_F)\boldsymbol{\alpha}+V_F(\boldsymbol{\varepsilon}-\mathbf{I}))\right]\cdot\hat{\xi}_l\right\}. \tag{37}$$

Our final result given in Eq. (37) represents the entire contribution to the first-order Raman scattering cross section from Coulomb and phonon interactions (Deformation or Frölich). The cross section is given in terms of the individual processes as well as their cross terms. In the limit of pure Deformation or Coulomb interaction, Eq. (37) reduces to the results given by Eqs. (27) and (28) or Eq. (36).

III. SCATTERING CROSS SECTION FROM PLASMA IN A MAGNETIC FIELD

In this section is discussed the Raman scattering cross section in solids under various conditions. Since we are concerned with the region $k/k_{FT}\ll 1$, we can neglect all k dependence in the electron dielectric tensor. First, we consider the scattering without magnetic field. The dielectric tensor is

$$\boldsymbol{\varepsilon}=[1-\omega_p^2/\omega(\omega-i\nu)]\mathbf{I}, \tag{38}$$

where $\omega_p^2=4\pi e^2 n/m^*\epsilon_\infty$ is the plasma frequency of the conduction electrons and ν is the collision frequency. Without loss of generality, we assume $\mathbf{k}\|\hat{x}$. Then, from Eq. (35), the cross section for the longitudinal mode, i.e., $\hat{\epsilon}_l\|\hat{x}$, can be written as

$$\left(\frac{d\sigma}{d\omega d\Omega}\right)_l = \frac{r_0^2}{2\pi}\frac{1}{e^{\beta\omega}-1}\frac{1}{4\pi} \times\text{Im}\left(\frac{[V_D^2\alpha\epsilon+V_F^2(\alpha+\epsilon-1)+2V_DV_F\alpha]}{\alpha+\epsilon}\right). \tag{39}$$

Near the resonance, i.e., $\epsilon+\alpha=0$, the cross section for

the case of $\nu=0$ reduces to

$$\left(\frac{d\sigma}{d\omega d\Omega}\right)_l=\frac{r_0^2}{2\pi}\frac{1}{e^{\beta\omega}-1}\frac{1}{4\pi}\times\left|V_D\left(1-\frac{\omega_p^2}{\omega^2}\right)+V_F\right|^2\mathrm{Im}\left(\frac{1}{\epsilon+\alpha}\right),\quad(40)$$

which is in agreement with the result obtained in Refs. 2, 12, and 14. The connection with Ref. 14 is obtained by using the identity

$$D(\mathbf{q},\omega)\equiv[2\omega_l/(\omega_t^2-\omega_l^2)]\times[\alpha/(1+\alpha)].$$

For realistic semiconductors, the phonon collision frequency η is of order $\eta=0.01\omega_t$ and much smaller than the electronic collision frequency ν when $\omega_p\sim\omega_t$. The phonon-collision frequency for coupled electron-phonon systems can be omitted provided the shift of the "renormalized phonon" frequency is larger than η, which is certainly the situation in our case. This point has been discussed in some detail in Ref. 14. For the transverse mode, for example, $\hat{\epsilon}_t\|\hat{y}$, the cross section becomes

$$\left(\frac{d\sigma}{d\omega d\Omega}\right)_t=\frac{r_0^2}{2\pi}\frac{|V_D|^2}{e^{\beta\omega}-1}\frac{1}{4\pi}\mathrm{Im}\left(\frac{\alpha(c^2k^2/\omega^2-\epsilon)}{c^2k^2/\omega^2-\epsilon-\alpha}\right).\quad(41)$$

This is the scattering cross section from "polariton." The scattered intensity from the transverse and longitudinal modes can be, in principle, quite different from one another. The intensity at the transverse phonon line (or, in the general case, the polariton) depends on V_D while the intensity at the longitudinal phonon line depends on both V_D and V_F. However, the intensity at the plasma line[2,14] depends mainly on V_F in the limit of no collisions.

In the following, we consider the light scattering from solids in the presence of a strong dc magnetic field (assume $\mathbf{H}_0\|\hat{z}$). Then, the electromagnetodielectric tensor becomes

$$\varepsilon=\begin{pmatrix}\epsilon_\perp & \epsilon_\times & 0\\ -\epsilon_\times & \epsilon_\perp & 0\\ 0 & 0 & \epsilon_{11}\end{pmatrix},\quad(42)$$

where

$$\begin{aligned}\epsilon_\perp&=1-\{\omega_p^2/[(\omega-i\nu)^2-\omega_c^2]\}[(\omega-i\nu)/\omega],\\ \epsilon_x&=i\omega_p^2\omega_c/[(\omega-i\nu)^2-\omega_c^2]\omega,\\ \epsilon_{11}&=1-\omega_p^2/\omega(\omega-i\nu).\end{aligned}\quad(43)$$

Here ω_c is the electron-cyclotron frequency. The lattice polarizability $\boldsymbol{\alpha}$ is unchanged in a magnetic field. The scattering cross section depends on the orientation of $\mathbf{k}$ and $\hat{\epsilon}_i$ with respect to the magnetic field.

For the case of $\mathbf{k}\perp\mathbf{H}_0$ (assume $\mathbf{k}\|\hat{x}$), we are interested in either $\hat{\epsilon}_i\|\hat{x}$ (longitudinal mode) or $\hat{\epsilon}_i\|\hat{y}$ (transverse mode). In the presence of a magnetic field, the plasmon mode is no longer pure longitudinal, but becomes partially transverse. Therefore, the cross section becomes more complicated. Their scattering cross sections are given, respectively, by

$$\left(\frac{d\sigma}{d\omega d\Omega}\right)_{\perp l}=\frac{r_0^2}{2\pi}\frac{1}{e^{\beta\omega}-1}\frac{1}{4\pi}\times\mathrm{Im}(|V_F|^2\chi_F+|V_D|^2\chi_D+|V_DV_F|\chi_{DF}),\quad(44)$$

and

$$\left(\frac{d\sigma}{d\omega d\Omega}\right)_{\perp t}=\frac{r_0^2}{2\pi}\frac{1}{e^{\beta\omega}-1}\frac{|V_D|^2}{4\pi}\mathrm{Im}\chi_t,\quad(45)$$

where

$$\chi_F=\left[(\epsilon_\perp+\alpha-1)\left(\epsilon_\perp+\alpha-\frac{c^2k^2}{\omega^2}\right)+\epsilon_\times^2\right]\Big/\epsilon_T,\quad(46)$$

$$\chi_D=\alpha\left[\left(\epsilon_\perp+\alpha-\frac{c^2k^2}{\omega^2}\right)\epsilon_\perp+\epsilon_\times^2\right]\Big/\epsilon_T,\quad(47)$$

$$\chi_{DF}=2\alpha\left(\epsilon_\perp+\alpha-\frac{c^2k^2}{\omega^2}\right)\Big/\epsilon_T,\quad(48)$$

$$\chi_t=\alpha\left[(\epsilon_\perp+\alpha)\left(\epsilon_\perp-\frac{c^2k^2}{\omega^2}\right)+\epsilon_\times^2\right]\Big/\epsilon_T,\quad(49)$$

and

$$\epsilon_T=(\epsilon_\perp+\alpha)\left(\epsilon_\perp+\alpha-\frac{c^2k^2}{\omega^2}\right)+\epsilon_\times^2.\quad(50)$$

The dispersion relation is determined by the zeros of ϵ_T. The behavior of $(d\sigma/d\omega d\Omega)_{\perp l}$ and $(d\sigma/d\omega d\Omega)_{\perp t}$ will be studied in detail. There are four branches in the dispersion relation which will be identified as ω_i $(i=1,2,3,4)$. Here ω_1 represents the lowest branch which starts as a dressed photon at small k and asymptotically tends towards the frequency of the magnetoplasmon mode. At larger k, ω_2 is the polariton branch, ω_3 is the longitudinal optic phonon branch, and ω_4 is the dressed photon branch. The scattering cross sections are proportional to the residues at the poles, ω_i, which are given by

$$\begin{aligned}R_l^{Fi}&=\left\{\left[(\epsilon_\perp+\alpha-1)\left(\epsilon_\perp+\alpha-\frac{c^2k^2}{\omega^2}\right)+\epsilon_x^2\right]\left(\frac{\partial\epsilon_T}{\partial\omega}\right)^{-1}\right\}_{\omega=\omega_i},\\ R_l^{Di}&=\left\{\alpha\left[\left(\epsilon_\perp+\alpha-\frac{c^2k^2}{\omega^2}\right)\epsilon_\perp+\epsilon_x^2\right]\left(\frac{\partial\epsilon_T}{\partial\omega}\right)^{-1}\right\}_{\omega=\omega_i},\\ R_t^{Di}&=\left\{\alpha\left[(\epsilon_\perp+\alpha)\left(\epsilon_\perp-\frac{c^2k^2}{\omega^2}\right)+\epsilon_x^2\right]\left(\frac{\partial\epsilon_T}{\partial\omega}\right)\right\}_{\omega=\omega_i}.\end{aligned}\quad(51)$$

The dispersion relations and the corresponding residues R_l^{Fi}, R_l^{Di}, and R_t^{Di} (the cross section) are illustrated in Figs. 4(a)–4(c) for several different values of ω_c and ω_p. One notes that both the longitudinal and the transverse modes have the same dispersion relation. As ω_c approaches zero (no magnetic field), for large k, branches ω_1 and ω_3 become purely longitudinal and ω_2

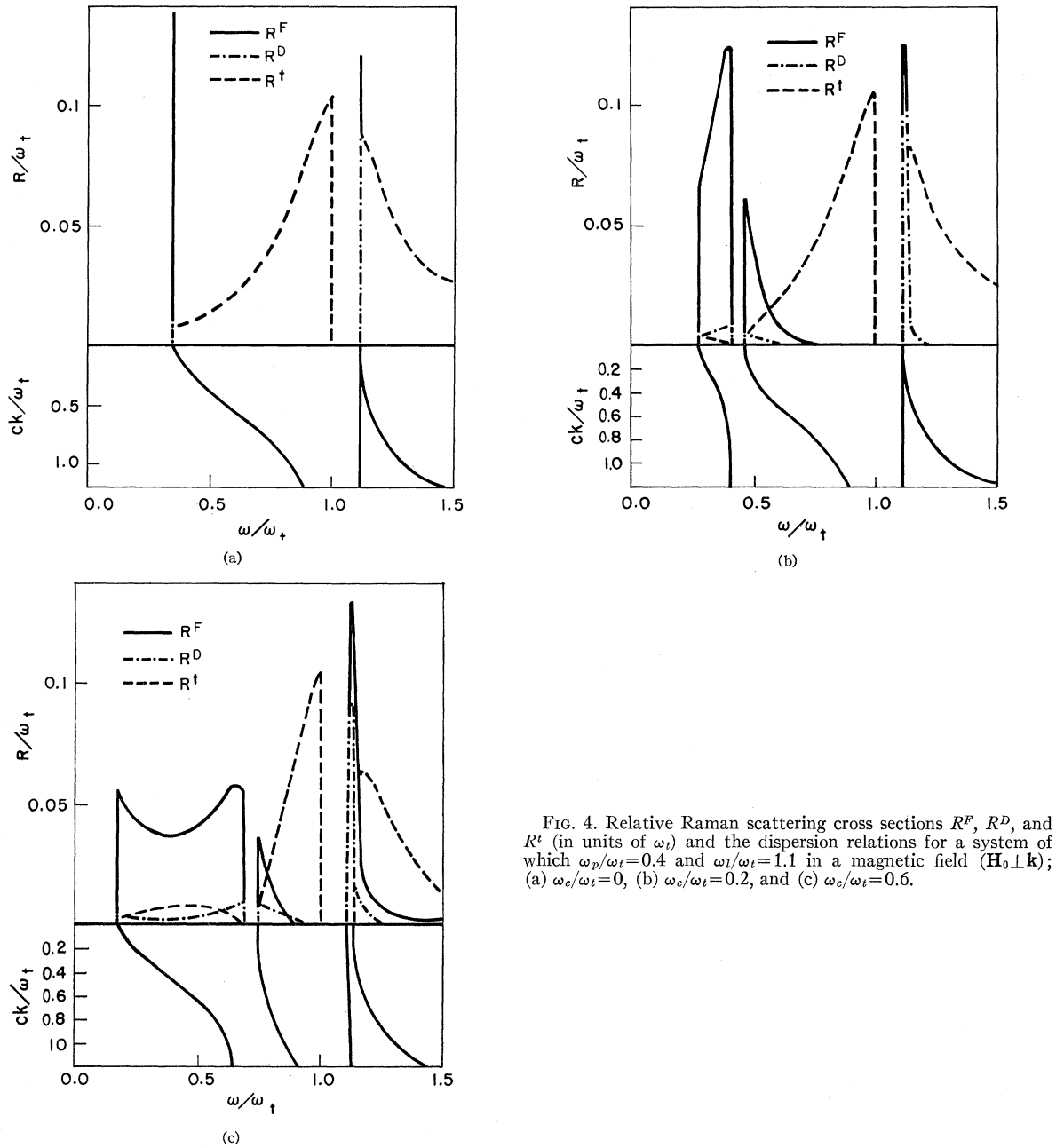

FIG. 4. Relative Raman scattering cross sections R^F, R^D, and R^t (in units of ω_t) and the dispersion relations for a system of which $\omega_p/\omega_t=0.4$ and $\omega_l/\omega_t=1.1$ in a magnetic field ($\mathbf{H}_0\perp\mathbf{k}$); (a) $\omega_c/\omega_t=0$, (b) $\omega_c/\omega_t=0.2$, and (c) $\omega_c/\omega_t=0.6$.

and ω_4 are purely transverse [see Fig. 4(a)]. This behavior is reflected in the residues R_l^{Fi}, R_l^{Di}, and R_t^{Di}. For $\omega_c=0$, R_l^{Fi} and R_l^{Di} are large at $i=1$, 3, which are pure longitudinal modes, and equal to zero for $i=2$, 4, which are purely transverse, and vice versa for R_t^{Di}. For finite ω_c, the longitudinal branches ω_1 and ω_3 and the transverse branches ω_2 and ω_4 are coupled together. All four branches are partially longitudinal and partially transverse. For small ω_c, the branches ω_1 and ω_3 are mainly longitudinal while the branches ω_2 and ω_4 are mainly transverse [see Fig. 4(b) for the case of $\omega_c=0.2\omega_t$]. As ω_c increases, the coupling between longitudinal and transverse modes becomes stronger [see Fig. 4(c) for the case $\omega_c=0.6\ \omega_t$]. One notes that scattering cross section due to Fröhlich coupling R_l^{Fi} is much larger than the cross section due to deformation potential R_l^{Di} near the plasmon frequency (or the magnetoplasmon frequency). This can be easily understood from Eq. (40) for the case of $\omega_c=0$. There, the cross section due to the deformation potential turns out to be proportional to $(1-\omega_p^2/\omega^2)^2$ in the collisionless case. This factor will reduce the scattering cross section

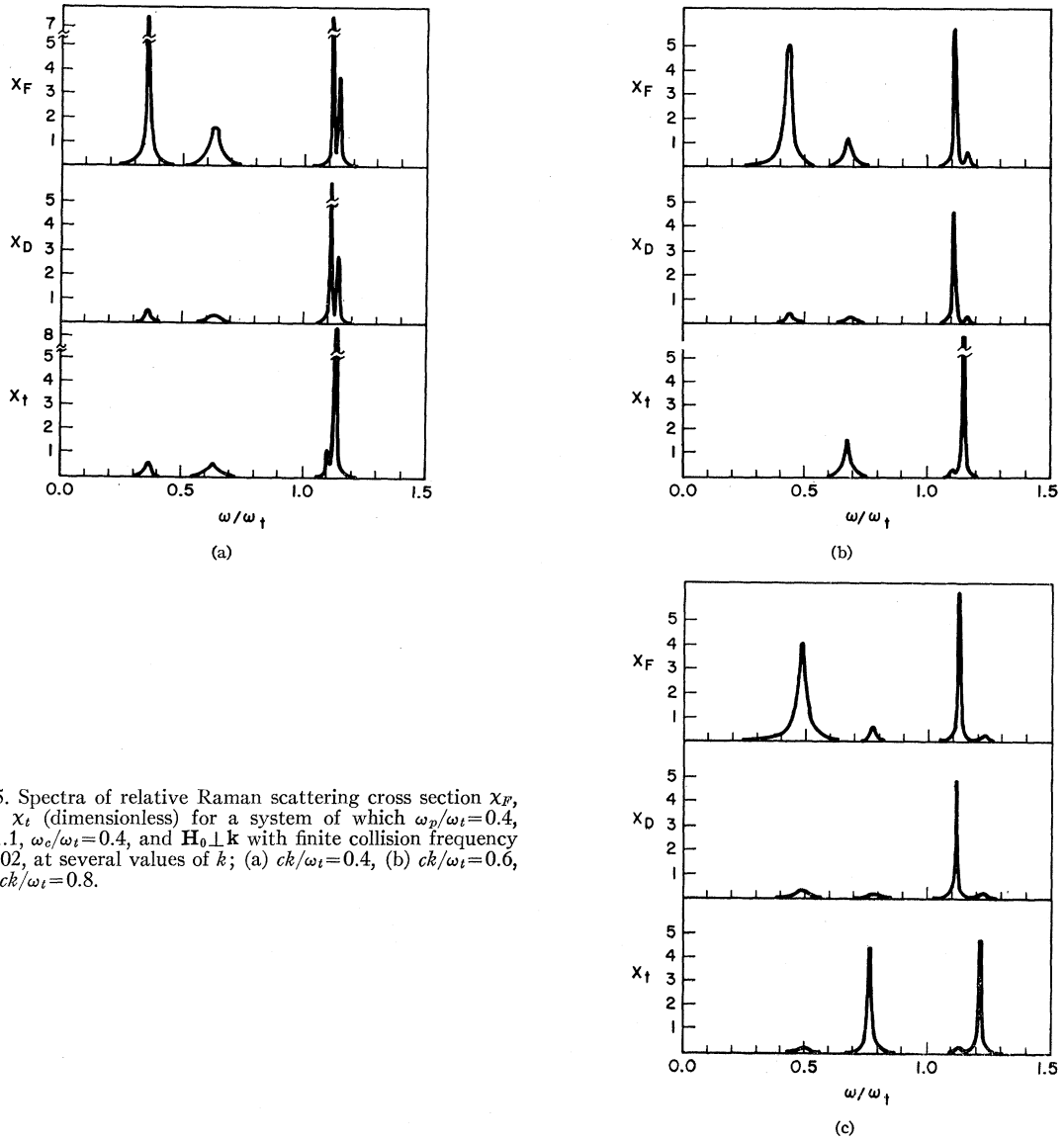

FIG. 5. Spectra of relative Raman scattering cross section χ_F, χ_D, and χ_t (dimensionless) for a system of which $\omega_p/\omega_t=0.4$, $\omega_l/\omega_t=1.1$, $\omega_c/\omega_t=0.4$, and $\mathbf{H}_0\perp\mathbf{k}$ with finite collision frequency $\nu/\omega_t=0.02$, at several values of k; (a) $ck/\omega_t=0.4$, (b) $ck/\omega_t=0.6$, and (c) $ck/\omega_t=0.8$.

severely near the plasmon frequency. From Figs.4(a)–4(c), one easily draws the following conclusion: In order to observe the scattering cross section from ω_1 and ω_3, the polarization vector should be so arranged that it will produce large longitudinal response (and vice versa for the transverse branches ω_2 and ω_4). Furthermore, in order to measure the plasmonlike branch ω_1, one needs a material having a larger Fröhlich coupling constant. In a real solid, the collision frequency ν is finite and one has to use Eqs. (44) and (45) to compute the cross section. The spectrum of the scattering cross section at several values of $\mathbf{k}$ are illustrated in Fig. 5(a)–5(c), with $\nu=0.05\omega_t$. One easily notes the difference between the cross section from the transverse modes (due to deformation potential) and the longitudinal modes (due to deformation potential and due to Fröhlich coupling). In Figs. 5(a)–5(c), one sees that the resonance frequencies corresponding to different branches vary with the wave-vector transfer $\mathbf{k}$ and the strength at the resonances also vary from longitudinallike to transverse-like modes and from deformation potential to Fröhlich-coupling–caused scattering. The Fröhlich-coupling–caused scattering yields the largest cross section for the plasmonlike branch. The reported experiment[4] only measured the polaritonlike branch but failed to see the plasmonlike branch in a magnetoplasmon-phonon system. As we have discussed, in order to observe the plasmonlike branch, one needs a material with large Fröhlich-coupling constant and the polarizations should be so arranged that they produce a large scattering from longitudinal modes.

For the case of $\mathbf{k}\|\mathbf{H}_0\|\hat{z}$, longitudinal modes and

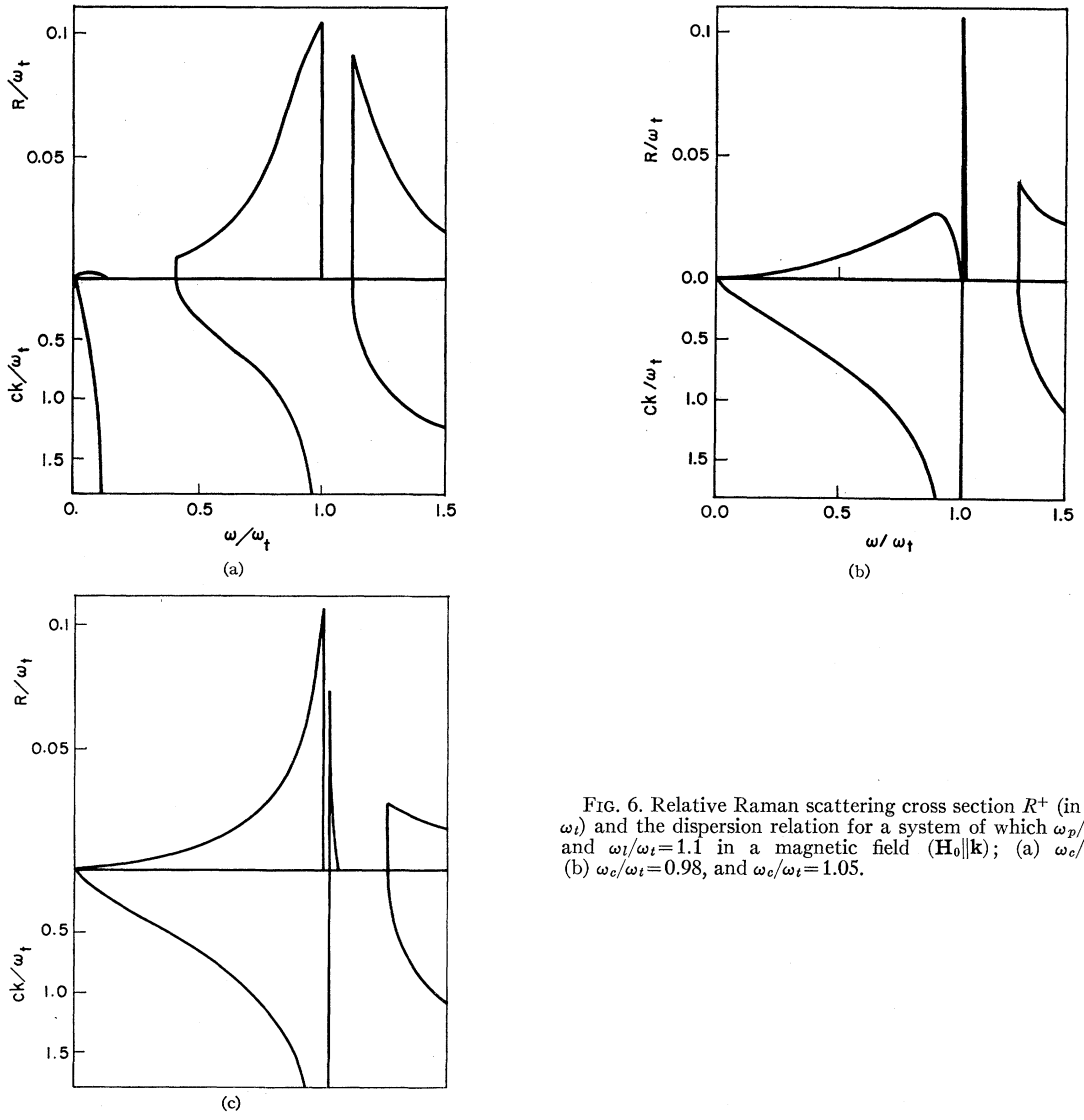

FIG. 6. Relative Raman scattering cross section R^+ (in units of ω_t) and the dispersion relation for a system of which $\omega_p/\omega_t=0.4$, and $\omega_l/\omega_t=1.1$ in a magnetic field ($\mathbf{H}_0\|\mathbf{k}$); (a) $\omega_c/\omega_t=0.1$, (b) $\omega_c/\omega_t=0.98$, and $\omega_c/\omega_t=1.05$.

transverse modes do not couple to each other. The longitudinal modes are not affected by the magnetic field $\mathbf{H}_0$. Therefore, we are mainly interested in the transverse modes which can be decomposed into two independent modes with respect to circularly polarized coordinates $(1/\sqrt{2})(\hat{x}+i\hat{y})$ and $(1/\sqrt{2})(\hat{x}-i\hat{y})$. The dielectric tensor becomes

$$\varepsilon=\begin{bmatrix}\epsilon_+ & 0 & 0\\ 0 & \epsilon_- & 0\\ 0 & 0 & \epsilon_{11}\end{bmatrix}, \tag{52}$$

where

$$\epsilon_\pm=1-\omega_p{}^2/\omega(\omega-i\nu\mp\omega_c). \tag{53}$$

Here ϵ_+ and ϵ_- correspond, respectively, to the right-hand and left-hand polarized modes. Using Eq. (41), we obtain the scattering cross section as

$$\left(\frac{d\sigma}{d\omega d\Omega}\right)_\pm=\frac{r_0{}^2}{2\pi}\frac{|V_D|^2}{e^{\beta\omega}-1}\frac{1}{4\pi}\mathrm{Im}\chi_\pm, \tag{54}$$

where

$$\chi_\pm=\frac{\alpha(c^2k^2/\omega^2-\epsilon_\pm)}{c^2k^2/\omega^2-\alpha-\epsilon_\pm}. \tag{55}$$

Their dispersion relations are determined by the zeros of the denominators in Eq. (55) which can be written as (with $\nu=0$)

$$\epsilon_T=\frac{c^2k^2}{\omega^2}-\frac{\omega^2-\omega_l{}^2}{\omega^2-\omega_t{}^2}-\frac{\omega_p{}^2}{\omega(\omega\mp\omega_c)}. \tag{56}$$

The frequencies of the right-hand and the left-hand polarized modes are denoted, respectively, by ω_+ and ω_-. There are two branches in ω_-, which differ only quantitatively from the modes without magnetic field. For the right-hand polarized modes ω_+, there are three branches which are denoted by ω_1, ω_2, and ω_3, according

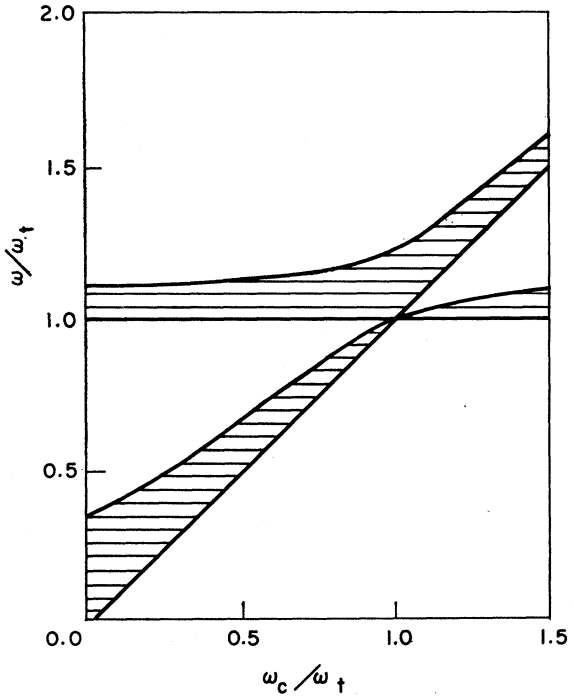

FIG. 7. Forbidden energy gap as a function of ω_c. The shaded areas represent the gap.

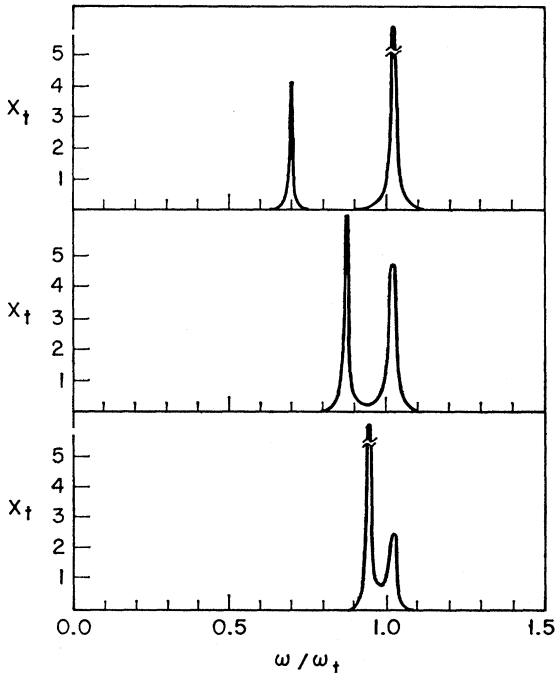

FIG. 8. Spectra of relative Raman scattering cross section χ^+ (dimensionless) for a system of which $\omega_p/\omega_t=0.2$, $\omega_l/\omega_t=1.1$, $\nu/\omega_t=0.02$, $\omega_c/\omega_t=1.05$, and $\mathbf{H}_0\|\mathbf{k}$, at several values of $\mathbf{k}$; $ck/\omega_t=1.0$, 1.5, 2.0.

to their energies. The frequency of ω_1 is zero at $k=0$ and approaches ω_c for large k. We will call it the cyclotron mode. The second mode ω_2 is the transverse phonon mode, the frequency of which approaches ω_t at large k. The third mode ω_3 is the photon mode, which behavse as a photon at large k. In the frequency region with $\omega\sim ck$, all three modes interact with each other, i.e., they are mixtures of photon, cyclotron mode, and transverse phonon. In the following, we will discuss ω_+ in detail. The scattering cross sections are proportional to the residues at the poles, ω_i, which are given by

$$R_\pm{}^i=\left[\alpha\left(\frac{c^2k^2}{\omega^2}-\epsilon_\pm\right)\left(\frac{\partial\epsilon_T}{\partial\omega}\right)^{-1}\right]_{\omega=\omega_i}. \qquad (57)$$

The dispersion relations ω_+ and the corresponding residues $R_+{}^i$ are illustrated in Figs. 6(a)–6(c) for several values of ω_c. For $\omega_c=0$ [see Fig. 6(a)], ω_+ is just the polariton, which has two forbidden energy gaps, i.e., from 0 to ω_p and ω_t to ω. For $\omega_c<\omega_t$, a new cyclotron mode ω_1 appears, which pushes the polariton mode ω_2 upward and narrows the band width of ω_2, as shown in Fig. 6(b). The intensity of ω_1 increases as ω_c approaches ω_t, and vanishes at ω_c. For $\omega_c>\omega_t$ [see Fig. 6(c)], the ω_1 mode becomes polaritonlike, but it starts at zero frequency at small k instead of ω_p, as in the case of $\omega_c=0$. The forbidden energy gaps are severely modified and shifted. The cyclotron mode may exist in the region between ω_t and ω_l. In Fig. 7, we illustrated the ω_c-dependent forbidden energy gap. The upper bounds of the forbidden energy gap are determined by the values of ω_2 and ω_3 at $k=0$. The lower bounds are determined by the values of ω_1 and ω_2 at $k=\infty$, which are ω_c and ω_t. The shaded areas in Fig. 7 represent the gaps. In the

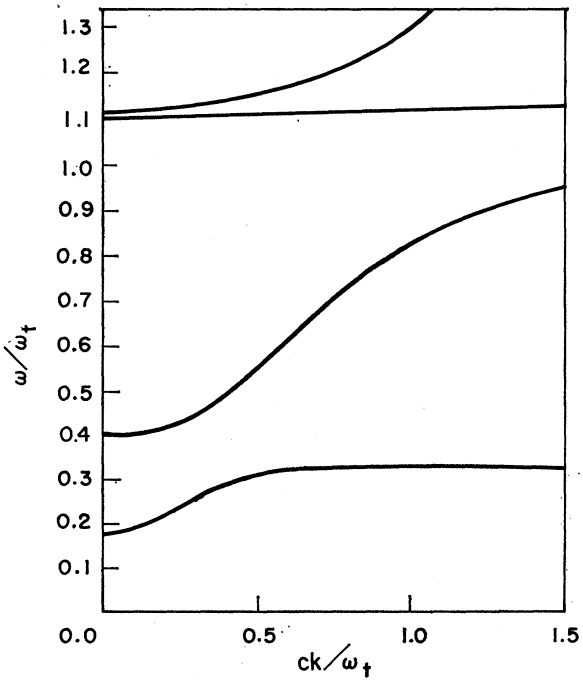

FIG. 9. Dispersion relation for an anisotropic electron gas. The wave-vector transfer $\mathbf{k}$ is in 1-2 plane and θ is the angle between k and axis -1. Here, $\cos^2\theta=0.6$, $\sin^2\theta=0.4$, $\omega_{p1}/\omega_t=0.4$, $\omega_{p2}/\omega_t=0.2$, and $\omega_l/\omega_t=1.1$.

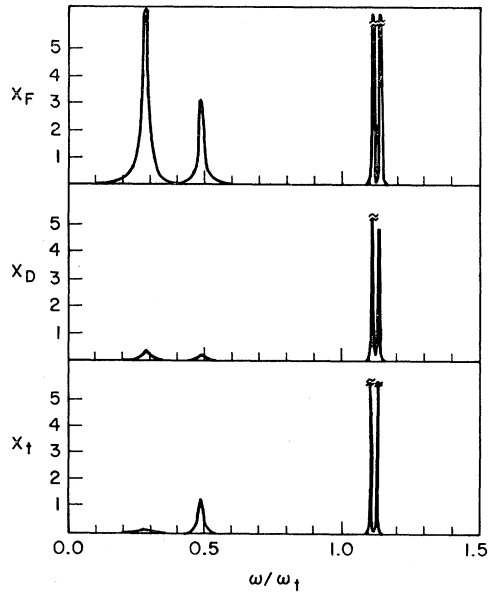

(a)

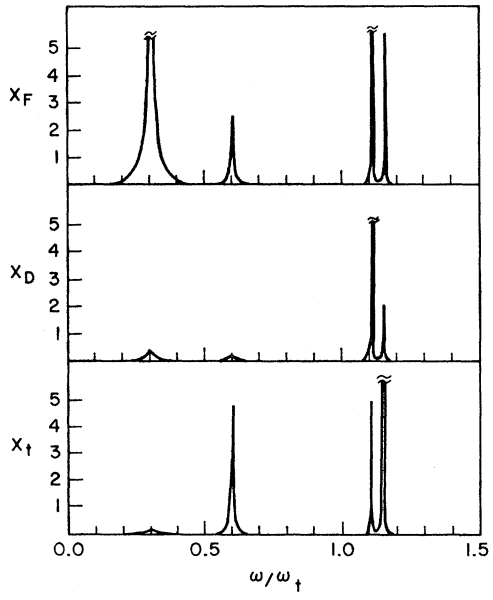

(b)

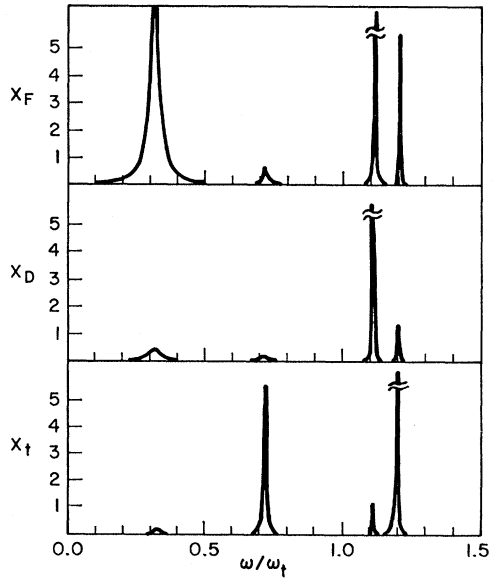

(c)

FIG. 10. Spectra of relative scattering cross section χ_F, χ_D, and χ_t (dimensionless), an anisotropic electron gas of which $\cos^2\theta=0.6$, $\sin^2\theta=0.4$, $\omega_{p1}/\omega_t=0.4$, $\omega_{p2}/\omega_t=0.2$, and $\omega_l/\omega_t=1.1$, at several values of k; (a) $ck/\omega_t=0.4$, (b) $ck/\omega_t=0.6$, and (c) $ck/\omega_t=0.8$.

limit of $\omega_c\gg\omega_t$, the system behaves as an empty lattice for $\omega\sim\omega_t$ and as free electrons for $\omega\gg\omega_t$. This can be easily seen from Eq. (56). Only in the region of $ck\sim\omega_t$, the forbidden energy gap is severely deviated from both the cases of free electrons and empty lattice. In Fig. 8, we show the scattering spectra for $\omega_c\sim1.05\omega_t$ in order to illustrate the coupling between the transverse phonon and the cyclotron modes. For $\nu=0.02\omega_t$, one can easily observe both modes up to $ck/\omega_t=2$. This phenomenon can be also studied by measuring the optical propagation and absorption coefficients, which will be presented in a subsequent paper.

IV. RAMAN SCATTERING CROSS SECTION FROM AN ANISOTROPIC ELECTRON GAS

In this section, we shall consider the forward Raman scattering cross section due to phonon fluctuation from an anisotropic electron gas. This problem has been treated by the authors[15] considering only contribution to the scattered intensity from electron-density fluctuation, which is smaller by a factor of $(k/k_{FT})^2$ than the intensity from phonon fluctuations. Here, we shall use the results of Sec. II [Eq. (35)] to an interacting system of phonons and an anisotropic electron gas. The dielec-

tric constant for an anisotropic electron gas (ellipsoidal Fermi surface) has the following form:

$$\varepsilon=\begin{bmatrix}\epsilon_1 & 0 & 0\\ 0 & \epsilon_2 & 0\\ 0 & 0 & \epsilon_3\end{bmatrix}, \tag{58}$$

where

$$\epsilon_i=1-\frac{{\omega_{pi}}^2}{\omega(\omega-i\nu)}, \quad i=1,2,3. \tag{59}$$

The wave-vector transfer $\mathbf{k}$ is assumed to be in 1-2 plane and the angle between $\mathbf{k}$ and axis -1 is θ. Substituting Eqs. (58) and (59) into Eqs. (27) and (37), we obtain the cross section as

$$\left(\frac{d\sigma}{d\omega d\Omega}\right)_l=\frac{{r_0}^2}{2\pi}\frac{1}{e^{\beta\omega}-1}\frac{1}{4\pi}$$
$$\times\mathrm{Im}(|V_F|^2\chi_F+|V_D|^2\chi_D+|V_DV_F|\chi_{DF}) \tag{60}$$

and

$$\left(\frac{d\sigma}{d\omega d\Omega}\right)_t=\frac{{r_0}^2}{2\pi}\frac{1}{e^{\beta\omega}-1}\frac{|V_D|^2}{4\pi}\mathrm{Im}\chi_t, \tag{61}$$

where

$$\chi_F=\left[-\left(\frac{c^2k^2}{\omega^2}-1\right)[\cos^2\theta(\epsilon_1+\alpha-1)+\sin^2\theta(\epsilon_2+\alpha-1)]\right.$$
$$\left.+(\epsilon_1+\alpha-1)(\epsilon_2+\alpha-1)\right]\Big/\epsilon_T, \tag{62}$$

$$\chi_D=\alpha\left[-\left(\frac{c^2k^2}{\omega^2}-\alpha\right)(\cos^2\theta\epsilon_1+\sin^2\theta\epsilon_2)+\epsilon_1\epsilon_2\right]\Big/\epsilon_T, \tag{63}$$

$$\chi_{DF}=2\alpha\left(\alpha+\epsilon_1\sin^2\theta+\epsilon_2\cos^2\theta-\frac{c^2k^2}{\omega^2}\right)\Big/\epsilon_T, \tag{64}$$

$$\chi_t=\left[-\left(\frac{c^2k^2}{\omega^2}+\alpha\right)(\epsilon_1\sin^2\theta+\epsilon_2\cos^2\theta+\alpha)\right.$$
$$\left.+(\epsilon_1+\alpha)(\epsilon_2+\alpha)\right]\Big/\epsilon_T, \tag{65}$$

and

$$\epsilon_T=-(c^2k^2/\omega^2)(\epsilon_1\cos^2\theta+\epsilon_2\sin^2\theta+\alpha)$$
$$+(\epsilon_1+\alpha)(\epsilon_2+\alpha). \tag{66}$$

The dispersion relation which is determined by $\epsilon_T=0$ is shown in Fig. 9. As was pointed out in our earlier paper,[15] for an anisotropic electron gas, the plasmon mode is no longer pure longitudinal but partially transverse and couples strongly to photon mode at $ck\sim\omega_p$. Here, we consider also the possibility of phonon fluctuations which couple to both photon and plasmon excitation modes and modify their dispersion relations. As illustrated in Fig. 9, there are four branches in the dispersion relation which can be labeled as

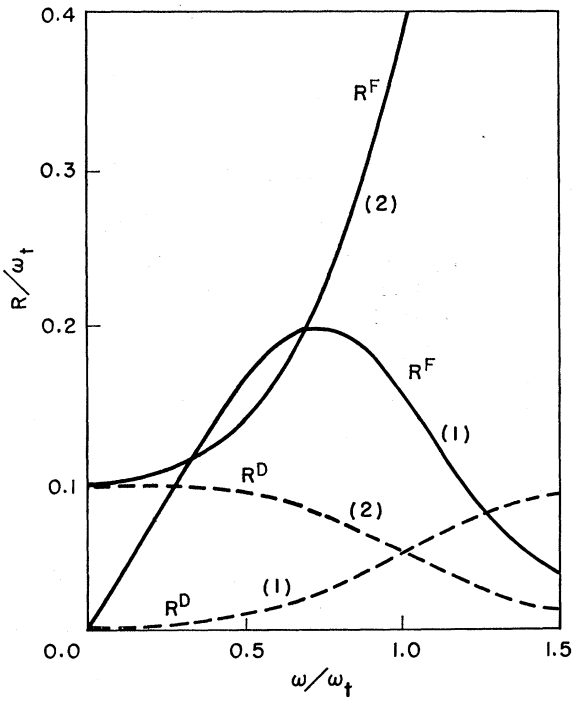

FIG. 11. Relative Raman scattering cross section R^F and R^D (in units of ω_t) from an electron-phonon system as a function of ω_p. The labels (1) and (2) indicate, respectively, the lower and the higher branches.

$\omega_i(i=1,2,3,4)$. Here, ω_1, which has the lowest energy, is the plasmonlike branch, ω_2 is the polaritonlike branch, ω_3 is the longitudinal-phononlike branch, and ω_4 is the photonlike branch. The spectra of the scattering cross section are illustrated in Figs. 10(a)–10(c) for several values of k. The Fröhlich coupling produced scattering given by χ_F and has the largest intensity at the plasmonlike branch ω_1, while χ_t has large intensity at the polaritonlike branch ω_2. The scattering intensity χ_D is small at ω_1 because it is proportional to the factor $(1-\omega_p^2/\omega^2)^2$. This point has been discussed in detail in Sec. III. In our earlier paper,[15] we pointed out that the plasmon frequency is shifted by coupling with photon, but the intensity is small and proportional to $(k/k_{FT})^2$. Here, the plasmon mode can have large intensity via its coupling to the phonons. In the following, we will discuss the relative scattering intensity between plasmon and phonon modes. For simplicity, we consider only the isotropic case which approximately gives us the relative intensities at the phonon and the plasmon resonant frequency. From Eq. (40), the coupled plasmon-phonon system has two modes, ω_1 and ω_2, which are determined by $\epsilon+\alpha=0$,

$${\omega_{1,2}}^2=\tfrac{1}{2}\{{\omega_p}^2+{\omega_l}^2\mp[({\omega_p}^2-{\omega_l}^2)^2$$
$$+4{\omega_p}^2({\omega_l}^2-{\omega_t}^2)]^{1/2}\}. \tag{67}$$

Here, ω_1 represents the lower mode and ω_2 is the higher mode. The scattering cross sections are proportional to

the residues at ω_1 and ω_2, which are given by

$$R^{Fi}=\left(\frac{\partial\epsilon_T}{\partial\omega}\right)_{\omega=\omega_i}^{-1},$$
$$R^{Di}=\left(1-\frac{\omega_p^2}{\omega_i^2}\right)^2\left(\frac{\partial\epsilon_T}{\partial\omega}\right)_{\omega=\omega_i}^{-1}. \tag{68}$$

The scattering intensity R^F and R^D are illustrated in Fig. 11. One notes that R^F and R^D behave quite differently. For $\omega_p<\omega_t$, R^{D1} is much smaller than R^{D2}, and, for $\omega_p>\omega_t$, R^{D2} is much smaller than R^{D1}. That means the scattering intensity, proportional to R^D, of the plasmonlike mode is much smaller than that of the phonon mode. The scattering intensity proportional to R_F for plasmonlike mode increases with ω_p, which has the same order of magnitude as the phononlike mode when $\omega_p\geq 0.3\omega_t$. Therefore, we can conclude that the anisotropic effects on the plasmon mode can be observable in forward scattering for systems with relatively large-Fröhlich-coupling constants.

V. DISCUSSION

We have considered the Raman scattering cross section for the "almost" forward direction in semiconductors. We calculate the scattering cross section arising from phonon fluctuations neglecting entirely scattering from electronic density fluctuations, which is negligible in our case. Our result indicates that scattering from the electronic longitudinal modes (plasmons) is possible provided the sample has substantial Fröhlich coupling. This might explain the result of Ref. 4 in which Patel and Slusher have observed the polariton mode in magnetic fields (which is mainly transverse) but could not observe the magnetoplasmon mode (which is mainly longitudinal). The scattering angle can be calculated, using conservation of energy and momentum, for given values of k_1, ω_1, k, and ω, and has been reported in literature.[11,15] We estimated for a realistic experimental situation with $\omega_\perp=1\,\mu$, one can observe a frequency shift of the polariton branch of the order $\frac{1}{10}\omega_t$ from the transverse-phonon frequency ω_t at a forward scattering angle between 0° and 2°.